

## Geostatistical scaling of canopy water content in a California salt marsh

E.W. Sanderson<sup>1</sup>, M. Zhang<sup>1</sup>, S.L. Ustin<sup>1</sup> and E. Rejmankova<sup>2</sup>

<sup>1</sup>Department of Land, Air, and Water Resources, University of California, Davis, CA 95616, U.S.A.; <sup>2</sup>Division of Environmental Studies, University of California, Davis, CA 95616, USA

(Received and accepted 2 July 1997)

**Key words:** geostatistics, scaling, grain, extent, canopy water content, salt marsh, remote sensing, Airborne Visible/Infrared Imaging Spectrometer (AVIRIS)

### Abstract

Remote sensing data are typically collected at a scale which is larger in both grain and extent than traditional ecological measurements. To compare with remotely sensed data on a one-to-one basis, field measurements frequently must be rescaled to match the grain of image data. Once a one-to-one correspondence is established, it may be possible to extrapolate site based relationships over a wider extent. This paper presents a methodology for rescaling the grain of ecological field data to match the grain of remotely sensed data and gives an example of the method in verification of remote sensing estimates of canopy water content in a tidal salt marsh. We measured canopy water content at 169 points on a semi-regular grid in the Petaluma Marsh, CA. A variogram describing the spatial correlation structure of the canopy water content was calculated and modeled. Ordinary kriging estimates of the canopy water content were calculated over blocks corresponding to image pixels acquired by the Airborne Visible/Infrared Imaging Spectrometer (AVIRIS). A water content index was determined from the reflectance data by calculating the area of a water absorption feature at 970 nm. A regression developed between the blocks and the pixels at the site was extrapolated over the image to obtain an estimate of canopy water content for the entire marsh. The patterns of canopy water content at the site and landscape levels suggest that different processes are important for determining patterns of canopy water content at different spatial extents. The errors involved in the rescaling procedures and the remote sensing interpretation are discussed.

### Introduction

Remote sensing is an important tool for ecologists attempting to understand ecological patterns and processes at landscape scales (Ustin et al., 1993; Wessman, 1992; Quattrochi and Pelletier, 1991) and is commonly used in landscape studies (O'Neill et al., 1996; Barkhadle, et al., 1994; Iverson et al., 1994; Knight et al., 1994; Haines-Young, 1992), however remote sensing provides information at a scale larger in grain and extent (*sensu* O'Neill et al., 1986) and of different kind (reflected light vs. direct measures of ecological phenomena) than most other ecological observations. Because of these differences in scale and kind, it is often difficult to separate the uncertainties due to the remote sensing interpretation from uncertainties due to

mismatches in scale when image data and field data are compared (Verstraete et al, 1996; Raffey, 1994a,b).

To separate these uncertainties, it is necessary to adopt some kind of scaling methodology to aggregate the field data, collected at a smaller grain, to the grain of the remotely sensed pixel, and estimate the aggregation error. Separate comparison of the rescaled ground data to the interpreted value of the pixel allows verification of the remote sensing interpretation. If a satisfactory relationship is found, another rescaling operation may be required, extrapolating the relationship from the extent of the original field site (typically smaller than the image) to the extent of the landscape observed by the image. Further verification (*sensu* Mankin et al., 1975) is usually required.

Many landscape ecologists face the dilemma of

how to compare datasets collected at different scales, which has led to many investigations of the effect of scale on sampling (Fuhlendorf and Smeins, 1996; Qi and Wu, 1996; McNaughton and Jarvis, 1991; Musick and Grover, 1991; Turner et al., 1991; Woodcock and Strahler, 1987) and of ecological scaling methodologies (Moody and Woodcock, 1995; Allen et al., 1993; Rastetter et al., 1992; Vitousek, 1991; Waring, 1991; Weins, 1989; O'Neill et al., 1986; Gardner et al., 1982). Most of these studies have found that the spatial scale of sampling has an important influence on the observed pattern, but have yet to find any general scaling rules for ecological phenomena (Jelinski and Wu, 1996; Levin, 1992).

Geostatistics has been used frequently in ecology and remote sensing, both for interpolation (Rossi et al., 1994; Atkinson et al., 1994; Van Der Meer, 1994; Atkinson et al., 1992; Rossi et al., 1992) and scale detection (Schlesinger et al., 1996; Hyppanen, 1996; Jackson and Caldwell, 1993; Legendre and Fortin, 1989; Curran, 1988). This paper advances the idea that geostatistics is also a useful scaling methodology. Based on the statistical properties of point scale measurements, geostatistics allows the investigator to estimate the value of a phenomenon at arbitrarily determined locations within the study site, with the goal of substantially increasing the number of observations at the point scale which can be compared to each area measurement. These point estimates can be aggregated at whatever grain and extent the investigator chooses, subject to the limits of the original grain and extent of the point measurements. Thus the investigator determines the scale to which the point estimates will be aggregated from a continuous range of possible scales and can precisely match them to the larger scale. Geostatistics works by estimating the spatial structure of a phenomenon (variogram analysis), then making an unbiased linear estimate (Issaks and Srivastava, 1989) of the value of the phenomenon at any point within the original study extent (kriging). The variogram guides the estimation process by assigning weights based on the modeled spatial autocorrelation. Further geostatistical algorithms allow for quantification of expected error in the estimates.

This paper shows how ecological field measurements were rescaled to match remotely sensed observations by applying geostatistics to data from a tidal salt marsh. Point measurements of canopy water content made over one sampling site were rescaled to the grain of image data (pixels from the Airborne Visible/Infrared Imaging Spectrometer (AVIRIS)) using

variogram analysis and kriging. Once a relationship was established over the extent of the study site, the relationship was rescaled a second time, by extrapolating from the extent of the site to the extent of the landscape. This second rescaling was verified at a second, independent reference site.

## Methods

### *Study area*

The observations for this study were made in a tidal salt marsh (Petaluma Marsh) along the Petaluma River, about 8 km from the mouth of the river in San Pablo Bay, CA (Figure 1). This marsh is part of a semi-contiguous network of tidal wetlands that stretch along the northern shore of San Pablo Bay and is part of the greater San Francisco Bay Estuary (Josselyn, 1983). Petaluma Marsh is constrained by levees along the Petaluma River to the east and south, and by rising topography on its western margin.

The vegetation of Petaluma Marsh is dominated by *Salicornia virginica*, a succulent halophyte with high canopy water content. Two other species grow in zones parallel to the Petaluma River: *Spartina foliosa*, a halophytic cordgrass (Mahall and Park, 1976), and *Scirpus robustus*, a meso-halophytic bulrush (Ustin et al., 1981). Both of these are less succulent than *Salicornia virginica* and have lower water content (Zhang et al., 1997). A suite of other species grow along the banks of natural channels in the marsh. These species include *Frankenia salina*, *Jaumea carnosa*, *Grindelia cuneifolia*, and *Lepidium latifolium*. Through the remainder of the paper, each species will be referred to by its generic name. All plant names follow the nomenclature of Hickman (1993).

Two sites were studied in the Petaluma Marsh. The first site (hereafter the River Site) was intensively sampled with the intention of developing a scaling relationship between field and remotely sensed measurements. The River Site covered a rectangular area (385 m by 175 m) parallel to the Petaluma River, including stands of *Spartina* and *Scirpus*, as well as large areas of *Salicornia*, and a small channel network (Figure 2). A second site, the Pond Site, was located in the interior of the marsh, approximately 1.2 km from the Petaluma River, beside several salt ponds or pans. The vegetation at the Pond Site was dominated by *Salicornia*. This site was used to verify extrapolated predictions of canopy water content based on the River Site results.

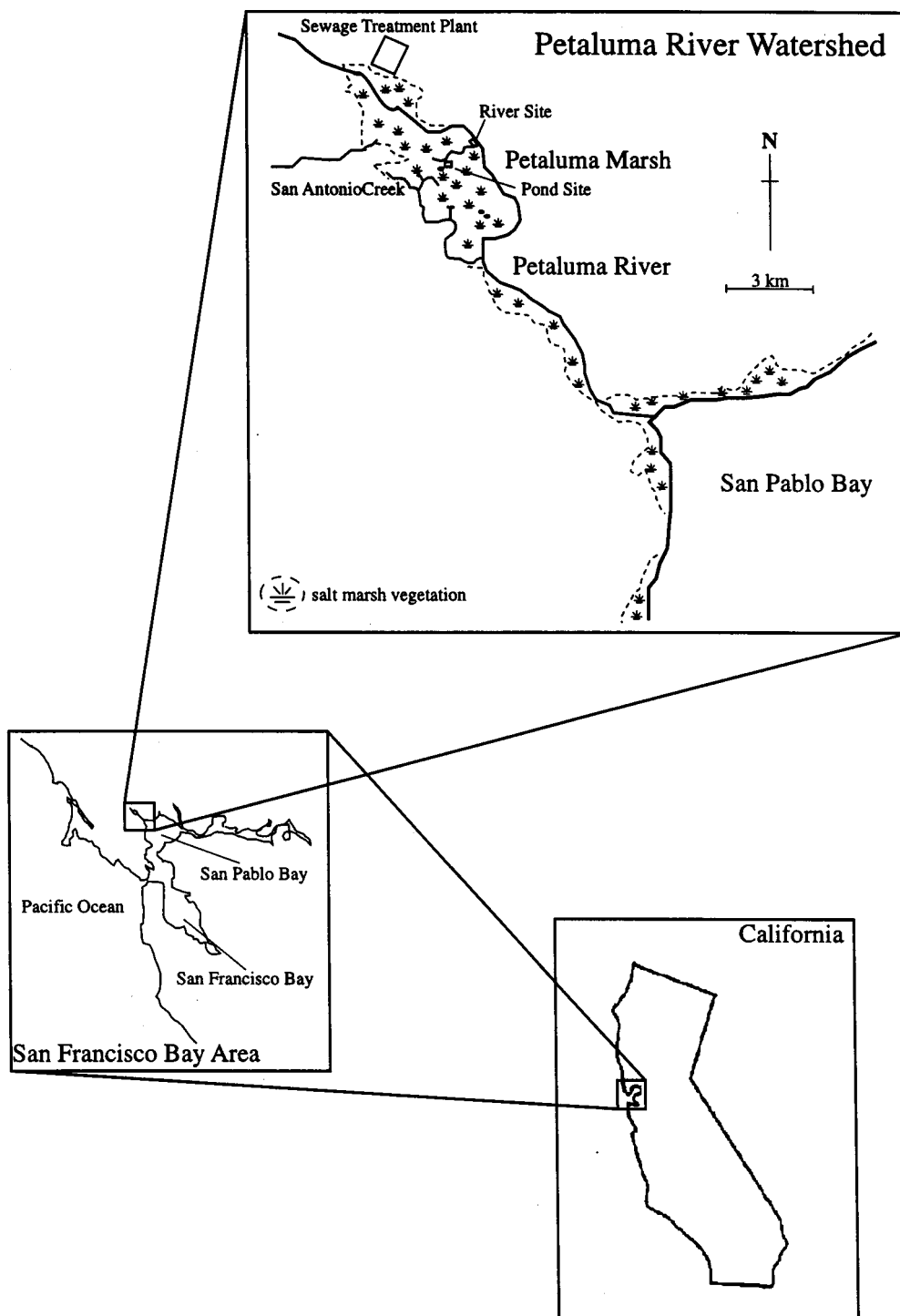


Figure 1. Study location in the Petaluma River watershed, the San Francisco Bay Estuary, and California.

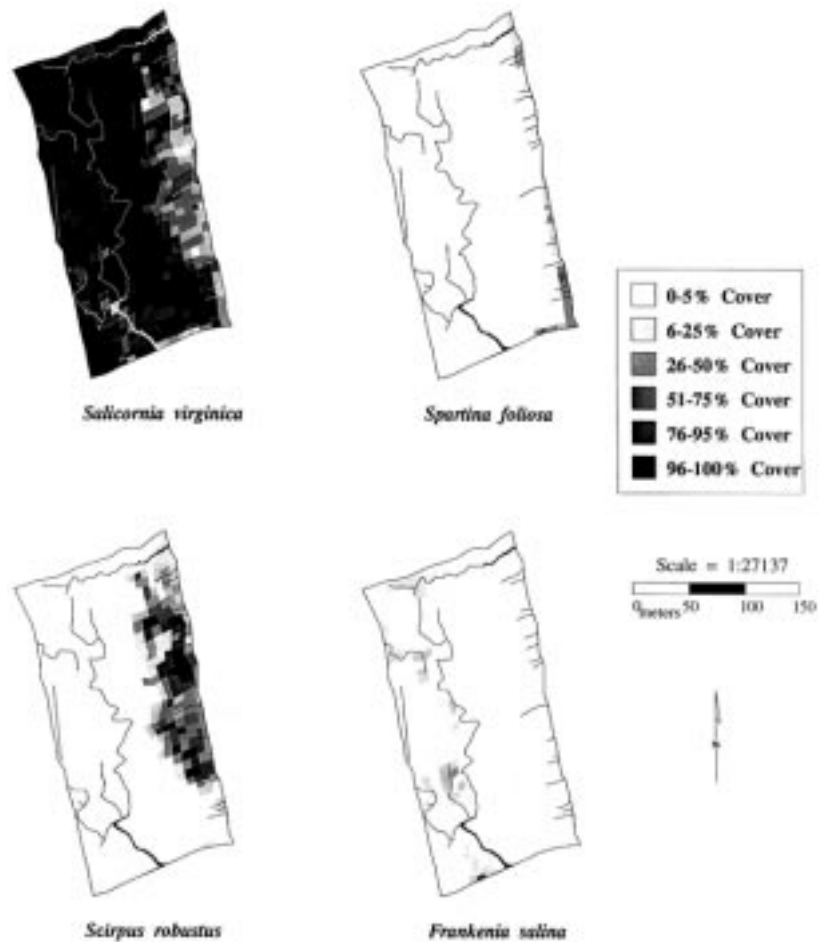


Figure 2. Vegetation distributions of *Salicornia virginica*, *Spartina foliosa*, *Scirpus robustus*, and *Frankenia salina* at the River Site, Petaluma Marsh. Cover estimates made over approximately 7.5 m by 7.5 m areas in the field.

### Sampling design

Canopy water content was selected for study because it has a strong influence on the spectral reflectance of vegetation (Lillesand and Kiefer, 1987) and because it is highly correlated with standing biomass (Zhang et al, 1997), and therefore, related to productivity. Moreover since all plants have a canopy water content, it is a continuous phenomenon which crosses spatial discontinuities in species distributions. Although the species are distributed in distinct zones, the study was designed to estimate canopy water content across the entire marsh, without previous knowledge of species locations, so all comparisons were made without respect to zonation.

At the River Site sample points were placed on an quasi-regular grid at approximately 15 m intervals (average nearest point-to-point distance was 12.3 m).

The sample spacing was chosen to underestimate the grain of AVIRIS data which nominally has 20 m square pixels. Canopy reflectance measurements and cover estimates by species were made at 169 sampling points on the grid. Canopy water determinations by destructive harvest were made at a subset of 38 points, stratified approximately equally in different species zones, following the other measurements. See Zhang et al. (1997) for methods. At the Pond Site fifteen sampling points were destructively harvested to determine canopy water content. All sampling at both sites was completed between May 15, 1994 and June 7, 1994 to coincide approximately with an AVIRIS overflight on May 21, 1994.

The location of each sampling point was determined as an average of ten measurements using a Pathfinder Plus Global Positioning System (GPS)

(Trimble Navigation, Sunnyvale, CA). In our study, GPS location measurements had a precision of 1–2 m (based on standard deviation of ten simultaneous measurements) and an accuracy of 3–10 m (based on repeated sampling at a later time.) Because of difficulties in processing the GPS measurements and satellite availability, twenty-two data locations were not measured directly, but had their position estimated relative to the other points. The accuracy for these points is somewhat less, but no worse than 15 m. The location of the natural channels and mosquito ditches were determined by mapping relative to the known sampling points.

#### *Canopy spectral measurements and analysis*

Upwelling canopy radiance was measured using an Analytical Spectral Devices Personal Spectrometer II (Analytical Spectral Devices, Boulder, CO) for the 345–1072 nm wavelength interval and with an approximately 2 nm spectral bandwidth. The fiber-optic head was suspended one meter above the canopy and oriented nadir. An 18° view restrictor was mounted on the optic to restrict the field of view to a circle of approximately 42 cm diameter (0.126 m<sup>2</sup>). At each sampling point, radiance measurements were collected in the visible and near-infrared regions separately and with different integration times, to maximize the signal-to-noise ratio of each measurement. Immediately before acquisition, incident radiation on the canopy was observed by measuring the upwelling radiance from a Spectralon white reflectance panel (Lab-sphere, Inc., North Sutton, NH) which is approximately 100% reflective for visible and near-infrared radiation. In post-processing the canopy radiance spectra were divided by the Spectralon panel radiance spectra to determine canopy reflectance (as a percentage of incident light). All radiance measurements were made between 1100 and 1500 hours PST. Reflectance spectra from each integration time were matched by making a least squares fit over the overlapping regions (approximately 850 to 900 nm), weighted by a running standard deviation five bands wide based on the shorter integration time spectra. This weighting function was used because the shorter integration time was optimized for measurement of upwelling radiance in the visible, which resulted in poor signal-to-noise in the near-infrared.

Canopy reflectance spectra were truncated to 400 to 1050 nm, averaged to 10 nm bands to correspond approximately to AVIRIS bands and normalized by

dividing by the square root of the sum of squared reflectance values for each spectra. While normalization minimized albedo variations in the reflectance spectra, it produced more consistency in the shape of the spectra, which is the focus of the remote sensing method used. Normalization over the entire spectrum has been suggested recently (Price, 1994; Pinzon, 1995) and is analogous to using NDVI (Normalized Difference Vegetation Index) instead of a simple ratio (Tucker, 1979).

Canopy water content was approximated from the reflectance spectra using a technique described as continuum removal (Clark and Roushe, 1984). This semi-empirical technique assumes a linear relationship between the area of an absorption feature and the chemical content that causes that absorption. A linear continuum is calculated over the wavelength interval of the feature to approximate a hypothetical reflectance in the absence of the feature. The area between the hypothetical reflectance and the measured reflectance is determined and compared to chemical content (in this case, canopy water content) to derive an empirical (linear regression) relationship (Zhang et al., 1997). This regression relationship was used to predict canopy water content at the 169 sampling points at the River Site.

#### *Variogram calculation and modeling and kriging estimation*

Observed variograms were calculated and modeled for the continuum removed area (CORA). A lag distance of 15 m and a width tolerance of 7.5 m, corresponding to the approximate spacing of the sample grid, gave the best resolved variogram, with each point on the variogram representing between 407 and 1321 data pairs (Figure 3). The search neighborhood was oriented roughly along the north-south axis, extending 0–100 m in the east-west direction and 0–200 m in the north-south direction to accommodate the rectangular area of the River Site. Directional variograms were also examined for evidence of anisotropy, but none was found.

We also calculated cross-variograms between canopy water content and CORA, but because of sparse water content sampling (38 points), those variograms had poorly defined structure. As a result, co-kriging approaches, which estimate water content directly, as suggested by Atkinson et al. (1992), gave poor estimations for our data set.

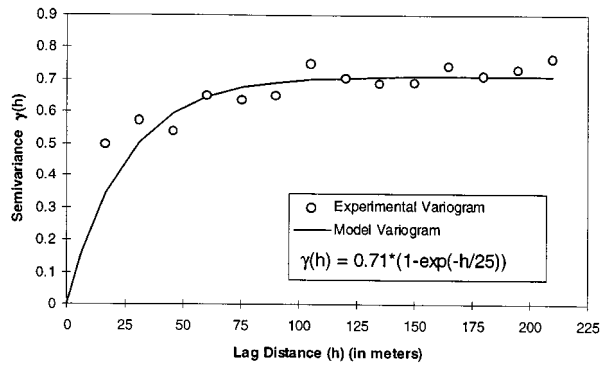


Figure 3. Observed variogram and exponential variogram model for canopy water content, based on spectral measurement (CORA), River Site, Petaluma Marsh.

The CORA observational variogram was modeled using an exponential model and no nugget (Figure 3). The range of the omnidirectional variogram model was 100 m with a sill equivalent to a canopy water content of 0.71 kg/m<sup>2</sup>. The nugget is defined as the semivariance at a lag distance of zero. Strictly the semivariance at lag zero should be zero; a nonzero nugget causes a discontinuity in the variogram which restricts the range of weighting values used in the estimation (Isaaks and Srivastava, 1989). Nonzero nuggets are often found in observed variograms and may indicate measurement error or short scale variability. In this study we attribute the nugget effect in the observed variogram to noise in the CORA estimates of canopy water content, so we did not include a nugget in the variogram model. See Atkinson et al., 1996, for further discussion on handling nugget effects in variograms calculated from remotely sensed data.

Ordinary kriging algorithms were used with the variogram model to estimate the canopy water content at a density of nine points per pixel, which was a marked increase over the original field data (an average 0.76 points per pixel, for the combined CORA and destructive harvests, or 0.14 points per pixel, for the destructive harvests only). Point estimates from the geostatistics were averaged (or “blocked”) to correspond to areas of the same size and location as the AVIRIS pixels.

Variogram modeling and kriging estimations were calculated using GEOPACK (Yates and Yates, 1989) and GEO-EAS (Englund and Sparks, 1988) software packages.

### Image acquisition and processing

A hyperspectral, visible and near-infrared image was acquired over the Petaluma River watershed by the Airborne Visible/Infrared Imaging Spectrometer (AVIRIS) (Vane et al., 1993) on May 21, 1994 at 13:19 PST. AVIRIS images are 512 pixels wide and 614 pixels long, with reflectance measured in 224, approximately 10 nm bands, covering the spectral range from 400–2500 nm. The instantaneous field of view of AVIRIS pixels is 20 m, but pixels overlap approximately 2.5 m on each edge, so that resolved pixels are approximately 17.5 m on a side. For 17.5 m pixels, the extent of the image is 8.96 km wide and 10.75 km long.

The image was calibrated to apparent surface reflectance using the Atmosphere Removal Program (ATREM, version 1.0) calibration algorithm (Gao et al., 1993). The calibration was optimized by adjusting the atmospheric calibration parameters and repetitively comparing calibrated pixel output to known ground spectra.

The calibrated image was viewed using the Spectral Image Processing System (SIPS) (Kruse et al., 1993) for analysis and interpretation. Using SIPS, we identified 16 bands in the near-infrared, from 918–1062 nm, which contained the 970 nm water absorption feature. These band reflectances were extracted from the image data cube to calculate the continuum removed area, using the same technique (Clark and Roushe, 1984) as described above for the canopy spectra. These steps were implemented using the Image Processing Workbench (Frew, 1990). The resulting one band image was imported in ARC/INFO and georeferenced using GPS acquired ground points at six road intersections on the image. The rectification error was less than 17.5 meters (i.e. one pixel) in both north-south and east-west directions.

The region of salt marsh vegetation was delineated by creating a mask from the AVIRIS band centered at 1222 nm, which gave the maximum contrast between the salt marsh vegetation and surrounding upland vegetation. This band was extracted from the data cube using SIPS, reformatted to a pixel grayscale map and contrast sharpened in XV, version 3.0 (John Bradley, Bryn Mawr, PA), then used as a mask in ARC/INFO. A second mask of the open water and channel network was prepared using the band centered at 1591 nm.

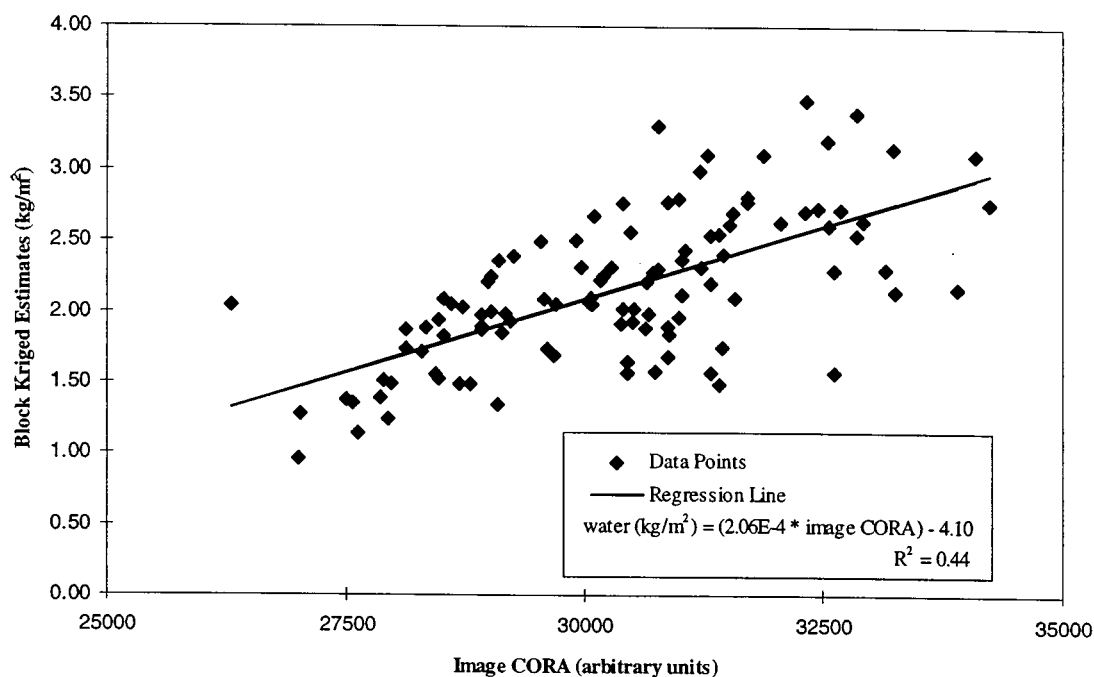


Figure 4. Scatterplot and regression of block kriged estimates to image derived measurements (CORA) of canopy water content at the River Site, Petaluma Marsh.

#### Comparison of ground observations to remote observations

Block kriged estimates and image measured canopy water content data were related by regression analysis (Figure 4). Because of extrapolation problems, edge pixels were not included in the regression relationship, resulting in a comparison of 157 pixels. This site-based regression relationship was applied across the entire image to estimate canopy water content values. Regression predictions of water content less than zero  $\text{kg/m}^2$  were set to zero  $\text{kg/m}^2$ . In general the pixels with less than zero  $\text{kg/m}^2$  (8.6% of total) corresponded to pixels lining the Petaluma River and tributaries, where pixels were not masked out because they included both vegetation and water elements.

#### Verification

The Pond Site destructive harvests were used to test the relationship between vegetation canopy water content and image CORA from the River Site. The predicted canopy water content map for the entire salt marsh was laid over an ARC/INFO coverage containing the Pond Site point sample data. Points were compared to

their corresponding pixels. Where two points fell in one pixel, the point values were averaged prior to comparison to the pixel value to avoid pseudo-replication. The point and pixel values were compared on a scatterplot and a regression line was calculated through the values (Figure 5). Three extreme values which were outside the range of canopy water content observed at the River Site were removed.

#### Results

The main quantitative results of this study are several distributions of canopy water content measured or estimated at different spatial grains and extents. Comparison of these distributions statistically and spatially constitutes the scaling framework used to extend the results from the site level to the landscape level. Examination of the statistics associated with each comparison allow us to estimate error for each scaling transformation.

The statistical distributions of canopy water content measured by destructive harvest and continuum removal (CORA) were similar but not identical. The univariate statistics of these distributions

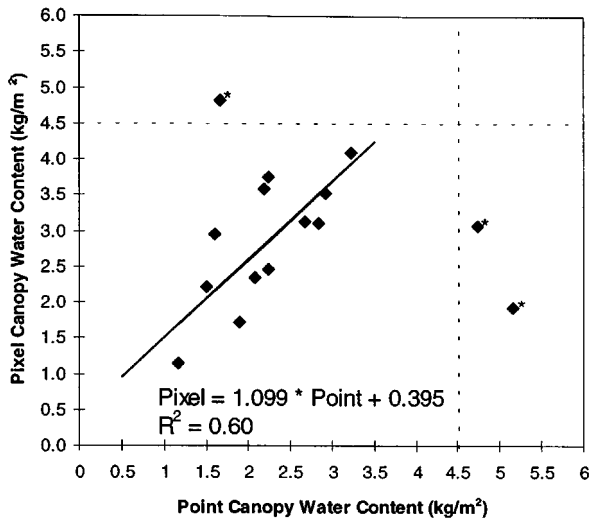


Figure 5. Scatterplot and regression of measured canopy water content to rescaled predictions of canopy water content at Pond Site, Petaluma Marsh.

(Table 1) showed similar means, but a higher maximum value and higher standard deviation associated with the destructive harvest data. The distribution of the destructive harvest data was negatively skewed because of disproportionate sampling of *Spartina*, which had a lower canopy water content, relative to *Spartina*'s areal coverage at the site. Although *Spartina* covers only approximately 1% of the sampled area (Figure 2), *Spartina* samples account for 26% of the destructive harvest water content observations.

The results of the kriging interpolation steps compared favorably with the ground measurements. The point kriged estimates were normally distributed with a mean identical to the mean CORA estimate of canopy water content, 2.08 kg/m<sup>2</sup> (Table 1), and with similar standard deviations (0.61 and 0.82 kg/m<sup>2</sup>), respectively; however, the overall range of the kriged distribution was contracted. Like most estimation algorithms, kriging tends to smooth the data.

The distribution of block kriged estimates was also normal with a slight increase in the mean compared to the point estimates, to 2.10 kg/m<sup>2</sup> (Table 1), with a standard deviation of 0.57 kg/m<sup>2</sup>. The extreme values were also truncated. In this case however the smoothing was not only a function of the kriging procedure, but also of the block averaging. Block averaging may be comparable to the smoothing due to pixel averaging by the sensor, and therefore not necessarily undesirable.

The block kriging estimates were very similar to the image-derived estimates (image CORA) of canopy water content. The block kriged estimate distribution (Table 1) was not statistically distinguishable from the image-derived distribution (Wilcoxon Rank Sum test ( $Z = -0.2872$ ;  $p = 0.7740$ )), though the image-derived distribution had a greater range and was less regular. Given that the distributions were approximately normal, we applied a Student's *t* test ( $t = 0.033$ ;  $p = 0.8552$ ) to show that means were also statistically indistinguishable (Table 1).

The spatial patterns of canopy water content through the various interpolation and averaging steps are shown in Figure 6. The original field measurements (Figure 6a), the estimation steps for points (Figure 6b) and blocks (Figure 6c), and the image data (Figure 6d), all show similar patterns. Lower canopy water content was observed in the *Spartina* and *Scirpus* zones, and higher water content in the *Salicornia* zone, particularly along the channel networks.

The relationship between block kriged canopy water estimates and image derived CORA data showed some scatter, but had a strong, linearly increasing trend (see Figure 4). The Pearson correlation coefficient ( $r$ ) between block and image derived water content estimates was 0.66. The regression equation had an  $R^2$  of 0.44 ( $p < 0.001$ ,  $n = 157$ ).

This site-based regression relationship was applied across the image to estimate the canopy water content distribution for the entire marsh landscape. The overall distribution was similar to the site level distribution, having similar mean and standard deviation (Table 1). The number of observations, however, was much larger ( $> 39,000$ ), and the range was wider, from 0–10.39 kg/m<sup>2</sup>. Zero values corresponded to areas of open or nearly open water which were not masked out by the channel mask. The shape of the distribution (not shown) was normal, but with a long, positively skewed tail of high values. We verified the landscape level results by comparing image derived estimates to point measurements made at the Pond Site. If the highest canopy water content values were omitted (points  $> 4.5$  kg/m<sup>2</sup>), then the regression showed an approximately linear relationship between pixel and point values at the Pond Site ( $R^2 = 0.60$ ;  $p < 0.003$ ,  $n = 12$ ) with a slope near one ( $m = 1.27$ ) (Figure 5).

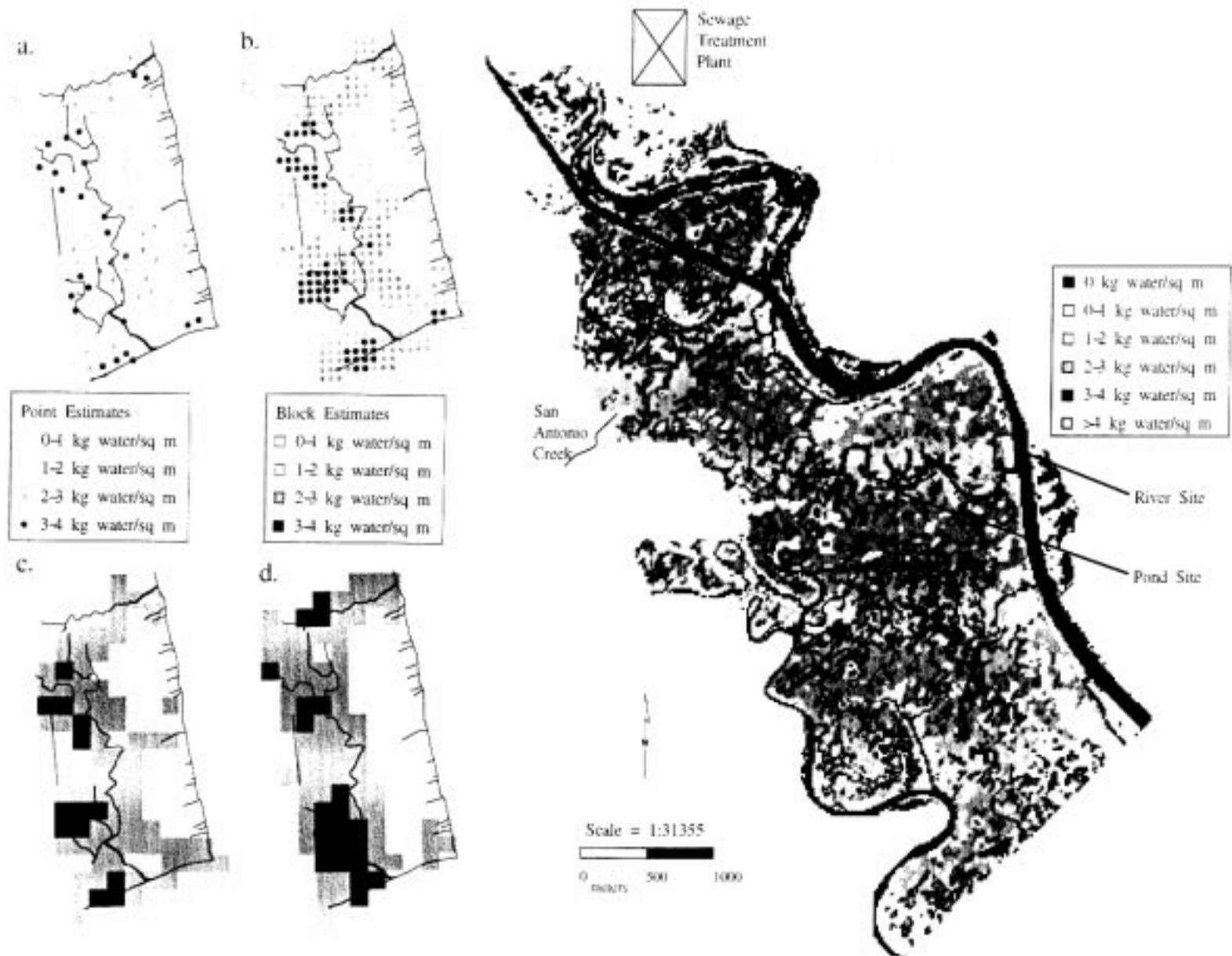


Figure 6. (left panel, a–d). Similarity of spatial patterns of observed and estimated canopy water content at the River Site, Petaluma Marsh. a. Spectral measurement (CORAs) of canopy water content; b. Point kriged estimates of canopy water content; c. Block kriged estimates of canopy water content; d. Image derived measurements of canopy water content. Figure 7. (right panel). Spatial pattern of canopy water content for Petaluma Marsh landscape.

Table 1. Similarity of statistical distributions of canopy water content ( $\text{kg}/\text{m}^2$ ) for field and image measurements and kriging estimates at River Site and across the Petaluma Marsh.

	Canopy water content at river site ( $\text{kg}/\text{m}^2$ )				
	Mean	Standard deviation	Minimum	Maximum	Number
Destructive harvest measurements	1.93	1.18	0.22	5.23	38
Spectral measurements (CORA)	2.08	0.82	0.20	3.93	169
Point kriged estimates	2.08	0.61	0.63	3.72	697
Block kriged estimates <sup>a</sup>	2.10 <sup>b</sup>	0.57	0.91	3.48	157
Remotely sensed observations <sup>a</sup>	2.12 <sup>b</sup>	0.80	0.26	3.99	157
	Canopy water content across marsh landscape ( $\text{kg}/\text{m}^2$ )				
Remotely sensed observations	2.37	1.34	0	10.39	39,282

<sup>a</sup>These distributions are statistically indistinguishable by Wilcoxon Rank Sum test ( $Z = -0.2872$ ;  $p = 0.7740$ )

<sup>b</sup>These means are statistically indistinguishable by Student's t test ( $t = 0.033$ ;  $p = 0.8552$ ).

## Discussion

### Site level pattern

The pattern of high and low canopy water content at the River Site suggested two casual processes (Figure 6d). The canopy water content bordering the Petaluma River, in the eastern third of the site, was generally low, in the 0–2  $\text{kg}/\text{m}^2$  range. In contrast the canopy water content away from the Petaluma River, in the western two-thirds of the site, was generally higher, in the 2–4  $\text{kg}/\text{m}^2$  range. The highest canopy water content values were associated with the tidal channel network in the center of the site.

Based on the spatial pattern of canopy water content, we hypothesized that the pattern was governed primarily by species distributions, and governed secondarily by the locations of tidal creeks, which may provide benefits to the neighboring vegetation (Zhang et al., 1997; Sanderson, in manuscript). Species distributions at the site were largely monotypic except immediately beside the channel networks and in the *Scirpus* zone, which was partially undergrown by *Salicornia* along its margins. *Salicornia* was clearly the dominant by area, covering 83% of the River Site (Figure 2). Areal percent coverage by other species declined sharply,

*Scirpus* 11%, *Frankenia* 1.5%, *Spartina* 1.3% and all other species less than 1% coverage.

These species differed in their canopy water contents (Table 2). The destructive harvests showed *Salicornia* had the highest canopy water content, consistent with its succulent leaves, followed by *Scirpus*, then *Spartina*; however the differences between *Scirpus* and *Spartina* were largely a function of phenology at sampling time. Neither were at peak biomass: *Scirpus* typically has more new biomass than *Spartina* by late May (Cameron, 1972). *Frankenia* had an intermediate canopy water content.

The second aspect of the pattern, higher water content associated with the channel network, can also be explained by the distribution and relative water content of plant species (Figure 2; Table 2). Several species (*Frankenia* is representative) are associated with the levees along the channel network, most which had healthy, green biomass at the time of sampling. These levee species are hypothesized to be associated with tidal channels because of tidal subsidies and reduced anoxia in the elevated sediments along the channel (Hinde, 1954). *Salicornia* near the channels may also benefit from tidal subsidies, causing them to grow more robustly than plants farther away, although we had too few points near the channels to confirm this pattern in our data.

Table 2. Distributions of canopy water content by species at River Site depend on observational method, either destructive harvests or spectral measurements (CORA).

Species*	Mean water content (kg/m <sup>2</sup> ), destructive harvest	N	Mean water content (kg/m <sup>2</sup> ), spectral interpretation (CORA)	N
All	1.93	38	2.05	169
Salicornia	2.56	21	2.32	124
Spartina	0.78	10	1.05	19
Scirpus	2.11	3	1.04	11
Frankenia	1.28	3	2.02	10
Other	1.71	1	1.56	4

\*Species estimated to have at least 50% of cover at that point, or in cases where total cover was less than 50%, species with highest cover by ocular estimate.

### Landscape level pattern

For most parts of the marsh, the pattern of species distribution and canopy water content suggested at the River Site are probably adequate to explain the spatial pattern of canopy water content for the marsh as a whole (Figure 7). Canopy water content seemed to be highest along small channels, and lower immediately along the Petaluma River and large sloughs, where *Spartina* and *Scirpus* grow. Although it is difficult to discern low-order channel networks in the image, elongate structures of higher water content are suggestive of channel network effects and correspond roughly to the locations of channels near the Pond Site.

For some localities, however, further explanations were needed to explain the pattern. For example, much higher water content was observed where San Antonio Creek, a fresh water stream, empties into the marsh in the northwest corner. Field reconnaissance after image analysis revealed large areas of upland, glycophytic species including *Lolium multiflorum* and *Poa annua*, and tall, lush broadleaf species lining the slough/creek in this area, including *Raphanus sativus* and one or more *Conium* spp. The biomass of these communities was probably higher on an area basis than the *Salicornia* dominated community characteristic of the main salt marsh, resulting in an apparently higher canopy water content, though we did not measure biomass or water content in this vegetation type. A series of abandoned fence posts demarcated the area, suggesting that at one time this portion of the marsh might have been reclaimed for pasture. The influx of freshwater from

San Antonio Creek may be maintaining non-halophytic species in this area.

In contrast low canopy water content was observed in a well-defined area neighboring the sewage treatment plant northeast of the river (Figure 7). Field reconnaissance of this area showed that levees define an area which receives fresh-water (treated) effluent from the treatment plant. As a result of the lower salinities and periodic flooding, several species typical of brackish marshes grow in this area including *Scirpus acutus* and *Typha* spp., in addition to large areas of the meso-halophytic *Scirpus robustus*. These plants grow in stands alternating with flooded areas, resulting in a patchwork of low to zero canopy water contents in this area.

Finally, an overall gradient in canopy water content is observable at the landscape level. It appears that canopy water content rises from the margins of the marsh from the Petaluma River to the interior, with the highest canopy water contents observed in the region where Zhang et al. (1997) reported a low growing, very dense form of *Salicornia*. This pattern is not observed in strip marshes along the Petaluma River or its tributaries, suggesting that some additional dynamic may be at work in the large, interior marsh which is not expressed in the smaller strip marshes.

### Landscape ecology and remote sensing: assessing errors

It is important when evaluating remotely sensed landscape patterns to remember what remote sensing data is: the measurement of reflected light from the landscape. In general, ecologists are not interested in reflected light per se, but in landscape properties (e.g. vegetation type) and/or processes (e.g. productivity) which may influence reflected light. Thus for remote sensing data to be useful, the radiance data must be transformed, through use of an interpretative technique, into a measure of the phenomenon of interest (Verstraete et al., 1996). For example in this paper, we use the continuum removal method to relate the area of a spectral feature to canopy water content. This semi-empirical interpretation had a measurable error at the point scale based on the fit of the regression line ( $R^2 = 0.63$ , from Zhang et al. (1997)) (Table 3). We desired to make a similar estimate of error at the pixel scale to verify our interpretation of the image data.

However evaluating the interpretation at the pixel scale is more difficult, because often we can not separate error in the interpretative methods from errors

Table 3. Estimation of error at different steps in the scaling procedure.

Procedural step	Unexplained variance	Suggested sources of error
Point scale spectral interpretation*	37%	Saturation; species specific canopy architecture and phenology
Grain to grain scale translation	9–63% (mean 14%)	Estimation of autocorrelation; modeling of autocorrelation
Block scale spectral interpretation	56%	Georeferencing; pixel sampling; atmospheric correction; errors from earlier steps.
Extrapolation of extent (verification at second site)	40%	Out of range; errors from earlier steps

\*From Zhang et al. (1997)

due to scale differences between the remotely sensed and field data (Verstraete et al., 1996). In fact, were we to compare the point measurements directly to image measurements, the observed error would subsume both interpretative and scaling errors. Combining these errors obscures both evaluation of the remote sensing method and the scaling procedure.

Our approach was to explicitly address and evaluate the scaling methodology separate from errors in remote sensing interpretation (Table 3). For the scaling methodology, kriging is advantageous because it allows estimation of the kriging variance at every point. In this example the kriging variances varied between 9–63%, with a mean variance of 14%. These variances measure the errors associated with the modeling of the autocorrelation structure (the variogram), the extent to which the distribution of canopy water content matched the assumptions of the kriging algorithms (stationarity and a normal distribution of the data), and the averaging of point estimates to pixel size areas. The criteria for evaluating the seriousness of these errors depends on the goals of the application, their magnitude and spatial distribution: here, the variances appeared to be randomly distributed spatially (not shown) and their magnitudes seemed reasonable, given known variances in the field measurements (37% unexplained variance) and errors in their locations.

The relative success of the scaling methodology provides additional information. Since kriging provided a satisfactory scaling method, we can infer that scaling of canopy water content met the assumptions of kriging as well, that is, canopy water content scales linearly over scales with grain from less than a square meter to over 300 m<sup>2</sup> and within an extent of approximately 67,000 m<sup>2</sup> (the River Site), despite spatial discontinuities due to species zonation. Moreover the canopy water content appears to be normally distrib-

uted over this range of scales. Canopy water content is autocorrelated at distances less than 100 meters, and the autocorrelation can be described using an exponential variogram model (Figure 3).

Although not perfect, these rescaled field measurements are at least known quantities, with known errors, which we can compare to the image. Like Zhang et al. (1997), we used linear regression to compare the remote sensing data to the field data, but here we compare them at the pixel scale (Figure 4). Scatter in this relationship ( $R^2 = 0.44$ ) derives from problems in georeferencing and registering, atmospherically correcting and then interpreting the image, as well as variance in the kriged field data. Despite all these potential errors, the statistical distributions of the rescaled field data and the image data are remarkably similar (Table 1). Thus the scatter probably results mostly from slight pixel to pixel discrepancies in the spatial distributions of the blocked data (Figure 6 c,d), related to georeferencing and registering of the image, and pixel sampling by the sensor. Recall that AVIRIS pixels overlap approximately 2.5 m on each edge.

The final step is to evaluate the remote sensing procedure when it is extrapolated beyond the primary site where it was developed, typically by making measurements at a second site. Here the regression at the Pond Site showed that the interpretation is satisfactory for canopy water content values within the same range as was observed at the River Site, but may be inadequate for predicting values outside that range ( $> 4 \text{ kg/m}^2$ ), which is consistent with deficiencies in both the scaling method (contraction of the distributions due to smoothing) and in the spectral interpretation (saturation of the water absorption feature) (Figure 5). Verifying the extrapolation informs us of the bounds of our interpretation at the landscape level. For example, predictions of canopy water content greater than 4 kg/m<sup>2</sup> are known

to be unreliable, based on the verification process, so they are uniformly color coded on Figure 7. Despite this kind of limitation on our analysis, a synthesis of field and remotely sensed data is the only tool we currently have to non-intrusively estimate canopy water content, and many other ecological properties, over landscape sized areas.

## Conclusion

This paper has shown a practical scaling strategy to relate ecological field data to a remote sensing image in order to verify and interpret landscape patterns. We showed that field measurements of canopy water content in a tidal salt marsh could be rescaled to remote sensing pixel estimates of the same parameter using geostatistics, and that the relationship obtained at the site level could be extended across the landscape. Preliminary analysis of the landscape pattern of canopy water content indicates processes at multiple scales are important for structuring the observed pattern. Errors due to the scaling procedure and the remote sensing interpretation were separately evaluated and used to inform the interpretation of pattern.

## Acknowledgments

The authors would like to acknowledge the following individuals for help in conducting field measurements: Claudia Castaneda, Larry Costick, Martha Diaz, John Gabriel, Quinn Hart, Robert Haxo, Helen Hansen, Han-Yu Hung, Stephane Jacquemoud, Kent Jorgensen, Alicia Palacios, Jorge Pinzon, Rebecca Post, George Scheer, Harry Spanglet, Lai-Han Szeto, Gail Wheeler, Linette Young, and QingFu Xiao. We additionally thank Harry Spanglet for comments on an earlier draft of this paper and for assistance with plant identifications, and Jorge Pinzon for many useful discussions. We wish to recognize the support of the US Environmental Protection Agency grant R82-1695-010 and the NASA EOS program under grants NAS5-31359 and NAS5-31714, and support for EWS under a NASA Global Change Fellowship, reference number 1995-GlobalCh00404. We also acknowledge the support of the Digital Equipment Corporation under a Sequoia 2000 grant for computer hardware.

## Disclaimer

This research was supported in part by grant R82-1695 from the US Environmental Protection Agency (EPA) – National Center for Environmental Research and Quality Insurance and in part by the US EPA Center for Environmental Health Research (R81-9658) at UC Davis. Although the information in this document has been funded wholly or in part by the US EPA, it may not necessarily reflect the views of the Agency and no official endorsement should be inferred.

## References

- Allen, T.F.H., A.W. King, B.T. Milne, A. Johnson, and S. Turner. 1993. The problem of scaling in ecology. *Evol. Trends in Plants* 7(1): 3–8.
- Atkinson, P.M., R. Dunn and A.R. Harrison. 1996. Measurement error in reflectance data and its implications for regularizing the variogram. *Int. J. Rem. Sens.* 17(8): 3735–3750.
- Atkinson, P.M., R. Webster and P.J. Curran. 1994. Cokriging with airborne MSS imagery. *Rem. Sens. Env.* 48: 1–25.
- Atkinson, P.M., R. Webster and P.J. Curran. 1992. Cokriging with ground-based radiometry. *Rem. Sens. Env.* 41: 45–60.
- Barkhadle, A.M.I., L. Ongaro and S. Pignatti. 1994. Pastoralism and plant cover in the lower Shabelle region, southern Somalia. *Landscape Ecol.* 9(2): 79–88.
- Cameron, G.N. 1972. Analysis of insect trophic diversity in two salt marsh communities. *Ecology* 53: 58–73.
- Clark, R.N. and T.L. Roushe. 1984. Reflectance spectroscopy: Quantitative analysis techniques for remote sensing applications. *J. Geophys. Res.* 89: 6329–6340.
- Curran, P.J. 1988. The semivariogram in remote sensing: an introduction. *Rem. Sens. Env.* 24: 493–507.
- Englund, E. and A. Sparks. 1988. GEO-EAS (Geostatistical Environmental Assessment Software) User's Guide. EPA600/4-88/033. Environmental Monitoring Systems Laboratory, Las Vegas, NV, USA.
- Frew, J.E. 1990 The Image Processing Workbench. Ph.D. dissertation, University of California, Santa Barbara, CA, USA.
- Fuhlendorf, S.D. and F.E. Smeins. 1996. Spatial scale influence on long-term temporal patterns of a semi-arid grassland. *Landscape Ecol.* 11(2): 107–113.
- Gao, B., K.B. Heidebrecht and A.F.H. Goetz. 1993. Derivation of scaled surface reflectances from AVIRIS data. *Rem. Sens. Env.* 44: 165–178.
- Gardner, R.H., W.G. Cale and R.V. O'Neill. 1982. Robust analysis of aggregation error. *Ecology* 63(6): 1771–1779.
- Haines-Young, R.H. 1992. The use of remotely-sensed satellite imagery for landscape classification in Wales (U.K.) *Landscape Ecol.* 7(4): 253–274.
- Hickman, J.C. 1993. The Jepson manual: higher plants of California. University of California Press, Berkeley, CA, USA.
- Hinde, H.P. 1954. Vertical distribution of salt marsh phanerogams in relation to tidal levels. *Ecol. Mon.* 24: 209–225.
- Hyppanen, H. 1996. Spatial autocorrelation and optimal spatial resolution of optical remote sensing data in boreal forest environment. *Int. J. Rem. Sens.* 17(17): 3441–3452.

- Issaks, E.H. and R.M. Srivastava. 1989. *An Introduction to Applied Geostatistics*, Oxford University Press, New York, NY, USA.
- Iverson, L.R., E.A. Cook and R.L. Graham. 1994. Regional forest cover estimation via remote sensing: the calibration center concept. *Landscape Ecol.* 9(3): 158–174.
- Jackson, R.B. and M.M. Caldwell. 1993. The scale of nutrient heterogeneity around individual plants and its quantification with geostatistics. *Ecology* 74(2): 612–614.
- Jelinski, D.E. and J. Wu. 1996. The modifiable areal unit problem and implications for landscape ecology. *Landscape Ecol.* 11(3): 129–140.
- Josselyn, M. 1983. *The Ecology of San Francisco Bay Tidal Marshes: a community profile*. US Fish and Wildlife Service, Washington, D.C. USA.
- Knight, C.L., J.M. Briggs and M.D. Nellis. 1994. Expansion of gallery forest on Konza Prairie Research Natural Area, Kansas, USA. *Landscape Ecol.* 9(2): 117–125.
- Kruse, F.A., A.B. Lefkoff, J.W. Boardman, K.B. Heidebrecht, A.T. Shapiro, P.J. Barloon and A.F.H. Goetz. 1993. The spectral image processing system (SIPS)-interactive visualization and analysis of imaging spectrometer data. *Rem. Sens. Env.* 44: 145–163.
- Legendre, P. and M.-J. Fortin. 1989. Spatial pattern and ecological analysis. *Vegetatio* 80: 107–138.
- Levin, S.A. 1992. The problem of pattern and scale in ecology. *Ecology* 73(6): 1943–1967.
- Lillesand, T.M. and R.W. Kiefer. 1987. *Remote Sensing and Image Interpretation*. John Wiley and Sons, New York.
- Mahall, B.E. and R.B. Park. 1976. The ecotone between *Spartina foliosa* Trin. and *Salicornia virginica* L. in salt marshes of northern San Francisco Bay. I. Biomass and production. *J. of Ecol.* 64: 421–433.
- Mankin, J.B., R.V. O'Neill, H.H. Shugart and B.W. Rust. 1975. The importance of validation in ecosystem analysis. In: *New Directions in the Analysis of Ecological Systems, Part 1*, George S. Innis, Ed., Simulation Councils Proceedings Series, Volume 5, Number 1, Simulation Councils, Inc., LaJolla, California
- McNaughton, K.G. and P.G. Jarvis. 1991. Effects of spatial scale on stomatal control of transpiration. *Agr. For. Met.* 54: 279–301.
- Moody, A. and C.E. Woodcock. 1995. The influence of scale and the spatial characteristics of landscapes on land-cover mapping using remote sensing. *Landscape Ecol.* 10(6): 363–379.
- Musick, H.B. and H.D. Grover. 1991. Image textural measures as indices of landscape pattern. In ed. Turner, M.G. and Gardner, R.H. *Quantitative Methods in Landscape Ecology*. Springer-Verlag, New York, NY, USA.
- O'Neill, R.V., D.L. DeAngelis, J.B. Waide and T.F.H. Allen. 1986. *A Hierarchical Concept of Ecosystems*. Princeton University Press: Princeton, NJ, USA.
- O'Neill, R.V., C.T. Hunsaker, S.P. Timmins, B.L. Jackson, K.B. Jones, K.H. Ritters and J.D. Wickham. 1996. Scale problems in reporting landscape pattern at the regional scale. *Landscape Ecol.* 11(3): 169–180.
- Pinzon, J.E., S.L. Ustin, Q.J. Hart, S. Jacquemoud and M.O. Smith. 1995. Using foreground-background analysis to determine leaf and canopy chemistry. In *Proc. 5th. Ann. JPL Airborne Earth Sci. Work.* Edited by R.O. Green. Jan. 23–27, 1995. Pasadena, CA, USA.
- Price, J.C. 1994. How unique are spectral signatures? *Rem. Sens. Env.* 49(3): 181–186.
- Qi, Y., and J. Wu. 1996. Effects of changing spatial resolution on the results of landscape pattern analysis using spatial autocorrelation indices. *Landscape Ecol.* 11(1): 39–49.
- Quattrochi, D.A. and R.E. Pelletier. 1991. Remote sensing for analysis of landscapes: an introduction. In ed. Turner, M.G. and Gardner, R.H. *Quantitative Methods in Landscape Ecology*. Springer-Verlag, New York, NY, USA.
- Raffey, M. 1994b. Heterogeneity and change of scale in models of remote sensing. *Spatialization of multi-spectral methods*. *Int. J. Rem. Sens.* 15(12): 2359–2380.
- Raffey, M. 1994a. Change of scale theory: a capital challenge for space observation of earth. *Int. J. Rem. Sens.* 15(12): 2353–2357.
- Rastetter, E.B., A.W. King, B.J. Cosby, G.M. Hornberger, R.V. O'Neill and J.E. Hobbie. 1992. Aggregating fine-scale ecological knowledge to model coarser-scale attributes of ecosystems. *Ecol. Appl.* 2(1): 55–70.
- Rossi, R., D. Mulla, A. Journel and E. Franz. 1992. Geostatistical tools for modeling and interpreting ecological spatial dependence. *Ecology* 62: 277–314.
- Rossi, R.E., J.L. Dungan and L.R. Beck. 1994. Kriging in the shadows: geostatistical interpolation for remote sensing. *Rem. Sens. Env.* 49: 32–40.
- Schlesinger, W.H., J.A. Raikes, A.E. Hartley and A.F. Cross. On the spatial pattern of soil nutrients in desert ecosystems. *Ecology* 77(2): 364–374.
- Tucker, C.J. 1979. Red and photographic infrared linear combinations for monitoring vegetation. *Rem. Sens. Env.* 8: 127–150.
- Turner, S.J., R.V. O'Neill, W. Conley, M.R. Conley and R.E. Humphries. 1991. Pattern and scale: statistics for landscape ecology. In ed. Turner, M.G. and Gardner, R.H. *Quantitative Methods in Landscape Ecology*. Springer-Verlag, New York, NY, USA.
- Ustin, S.L., R.W. Pearcy and D.E. Bayer. 1981. Plant water relations in a San Francisco Bay salt marsh. *Bot. Gaz.* 143(3): 368–373.
- Ustin, S.L., M.O. Smith and J.B. Adams. 1993. Remote sensing of ecological processes: a strategy for developing ecological models using spectral mixture analysis. In *Scaling Physiological Processes: Leaf to Globe*. pp. 339–357. Edited by J. Ehrlinger and C. Field. Academic Press, New York, New York, USA.
- Van Der Meer, F. 1994. Extraction of mineral absorption features from high-spectral resolution data using non-parametric geostatistical techniques. *Int. J. Rem. Sens.* 15(11): 2193–2214.
- Vane, G., R.O. Green, T.G. Chrien, H.T. Enmark, E.G. Hansen and W.M. Porter. 1993. The airborne visible/infrared imaging spectrometer (AVIRIS). *Rem. Sens. Env.* 44: 127–143.
- Verstraete, M.M., B. Plinty and R.B. Myneni. 1996. Potential and limitations of information extraction on the terrestrial biosphere from satellite remote sensing. *Rem. Sens. Env.* 58: 201–204.
- Vitousek, P.M. 1991. Global dynamics and ecosystem processes: scaling up or down? In Ehrlinger, J. and Field, C.B. *Scaling Physiological Processes: Leaf to Globe*. Academic Press, New York, NY, USA.
- Waring, R.H. 1991. How ecophysiologicals can help scale from leaves to landscapes? In Ehrlinger, J. and Field, C.B. *Scaling Physiological Processes: Leaf to Globe*. Academic Press, New York, NY, USA.
- Weins, J.A. 1989. Spatial scaling in ecology. *Func. Ecol.* 3: 385–397.
- Wessman, C.A. 1992. Spatial scales and global change: bridging the gap from plots to GCM grid cells. *Ann. Rev. Ecol. Sys.* 23: 175–200.
- Woodcock, C.E. and A.H. Strahler. 1987. The factor of scale in remote sensing. *Rem. Sens. Env.* 21: 311–312.
- Yates, S.R., and M.V. Yates. 1989. *Geostatistics for waste management: a user's manual for the GEOPACK Geostatistical Software System*. USDA Salinity Lab, Riverside, CA, USA.
- Zhang, M., S.L. Ustin, E. Rejmankova and E.W. Sanderson. 1997. Monitoring Pacific Coast Salt Marshes Using Remote Sensing. *Ecol. Appl.* 7(3): 1039–1053.